

Pillar[5]arene as a Co-Factor in Templating Rotaxane Formation

Chenfeng Ke,[†] Nathan L. Strutt,[†] Hao Li,[†] Xisen Hou,[†] Karel J. Hartlieb,[†] Paul R. McGonigal,[†] Zhidong Ma,[†] Julien Iehl,[†] Charlotte L. Stern,[†] Chuyang Cheng,[†] Zhixue Zhu,[†] Nicolaas A. Vermeulen,[†] Thomas J. Meade,[†] Youssry Y. Botros,^{‡,||} and J. Fraser Stoddart^{*,†}

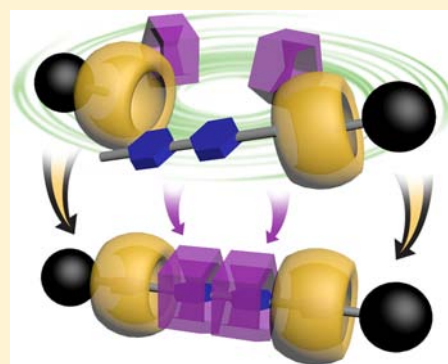
[†]Department of Chemistry, Northwestern University, 2145 Sheridan Road, Evanston, Illinois 60208, United States

[‡]Intel Laboratories, Building RNB-6-61, 2200 Mission College Boulevard., Santa Clara, California 95054-1549, United States

^{||}National Center for Nano Technology Research, King Abdulaziz City for Science and Technology, P.O. Box 6086, Riyadh 11442, Kingdom of Saudi Arabia

S Supporting Information

ABSTRACT: After the manner in which coenzymes often participate in the binding of substrates in the active sites of enzymes, pillar[5]arene, a macrocycle containing five hydroquinone rings linked through their *para* positions by methylene bridges, modifies the binding properties of cucurbit[6]uril, such that the latter templates azide–alkyne cycloadditions that do not occur in the presence of only the cucurbit[6]uril, a macrocycle composed of six glycoluril residues doubly linked through their nitrogen atoms to each other by methylene groups. Here, we describe how a combination of pillar[5]arene and cucurbit[6]uril interacts cooperatively with bipyridinium dications substituted on their nitrogen atoms with 2-azidoethyl- to 5-azidopentyl moieties to afford, as a result of orthogonal templation, two [4]rotaxanes and one [5]rotaxane in >90% yields inside 2 h at 55 °C in acetonitrile. Since the hydroxyl groups on pillar[5]arene and the carbonyl groups on cucurbit[6]uril form hydrogen bonds readily, these two macrocycles work together in a cooperative fashion to the extent that the four conformational isomers of pillar[5]arene can be trapped on the dumbbell components of the [4]rotaxanes. In the case of the [5]rotaxane, it is possible to isolate a compound containing two pillar[5]arene rings with local C₅ symmetries. In addition to fixing the stereochemistries of the pillar[5]arene rings, the regiochemistries associated with the 1,3-dipolar cycloadditions have been extended in their constitutional scope. Under mild conditions, orthogonal recognition motifs have been shown to lead to templation with positive cooperativity that is fast and all but quantitative, as well as being green and efficient.



1. INTRODUCTION

Complex biological molecules and assemblies are, more often than not, constructed under the guidance of nature's catalysts, the enzymes, which exploit noncovalent bonding interactions to recognize and bring together substrates with high specificities, lowering the transition state energies for the chemical reactions they catalyze. In certain cases, nonprotein molecules, known as cofactors, are necessary to trigger the activity of the otherwise latent enzymic machinery. Although the catalytic power of enzymes is rooted in a number of different phenomena operating in concert,¹ preorganization which orients the enzyme's active sites and substrates in space relative to each other is undoubtedly of paramount importance. Inspired by nature, chemists have developed elegant supramolecular systems which exploit noncovalent bonding interactions,² e.g., hydrogen bonding,³ hydrophobic forces,⁴ and van der Waals interactions⁵ to control the relative positioning of substrates in receptors. These systems, which act as simplified models of enzymes, can (i) accelerate reactions by increasing the effective molarity and/or preorganizing reactants, (ii) direct substrates along reaction paths which they would not otherwise follow, and (iii) discriminate between compounds bearing similar

functional groups as a consequence of selective binding.¹ Many successful designs utilize macrocyclic scaffolds such as cyclodextrins,⁶ crown ethers,⁷ metallocycles,⁸ calixarenes,⁹ and cucurbiturils¹⁰ as receptors to encapsulate substrates in their cavities, thus increasing the effective concentrations, and so accelerating the reaction.

Among these macrocyclic compounds, cucurbit[6]uril (CB) was first reported by Mock et al.¹¹ to act as a catalyst in the alkyne–azide 1,3-dipolar cycloaddition¹² (AAC), the Cu(I)-catalyzed variant of which has been popularized as the quintessential “click” reaction,¹³ giving rise to 1,4-disubstituted triazoles regioselectively with a considerable acceleration of the reaction rate, often ca. 10⁵-fold compared to the uncatalyzed reaction. Since its discovery by Mock, the CB-catalyzed 1,3-dipolar cycloaddition (CB-AAC) has found application in the construction of polymers,¹⁴ mechanically interlocked molecules (MIMs)¹⁵ and pH-responsive controlled-release systems.¹⁶

Despite the fact that both the CB-AAC and the Cu(I)-catalyzed cycloaddition (CuAAC) exhibit favorable kinetics and

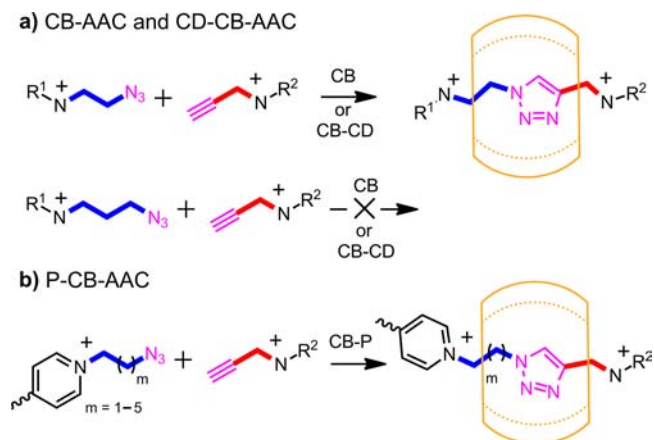
Received: July 15, 2013

Published: September 23, 2013

regiospecificities, the former has found comparatively few applications compared to the now ubiquitous CuAAC. Perhaps the fact that CB is not as freely available as copper salts and is less convenient to handle because of its poor solubility¹⁷ in water¹⁸ and other common laboratory solvents¹⁹ add up to explanations of a sort. The greatest drawback of the CB-AAC, however, is its substrate scope: *to date, all reports are restricted to describing reactions between propargylammonium and azidoethylammonium derivatives.* This limited scope can be rationalized by considering the cyclization mechanism and noncovalent bonding interactions which underpin the reaction. CB-AAC proceeds by means of the initial formation of a heteroternary complex, which renders the cyclization a pseudounimolecular process as a result of bringing the triple bond in the propargylammonium ion and the azide function in the azidoethylammonium ion into close proximity as well as aligning them so that they are poised to undergo triazole ring formation.^{11a,20} The entropic cost of bringing the CB and AAC precursors together is compensated²¹ for by the favorable binding enthalpy and the release of high energy water molecules from the cavity of the CB. Charge-dipole and hydrogen-bonding interactions between the secondary dialkylammonium ions and the carbonyl groups around the rim of the CB are maximized when the NH_2^+ centers are close to the planes of carbonyl oxygens, a requirement that dictates the geometry of the ternary complex. Consequently, altering the distance between the NH_2^+ centers and the alkyne/azide groups in the substrates disturbs the near-perfect alignment in the ternary complex, a geometry that is necessary in order to lower the transition-state energy of the AAC.²²

Recently, we developed a cooperative capture strategy^{23,24} for the assembly of MIMs that exploits the acceleration of the CB-AAC (Scheme 1a) in the presence of either β -cyclodextrin

Scheme 1. 1,3-Dipolar Alkyne–azide Cycloaddition Catalyzed by (a) a CB Ring or (b) a Combination of CB and CD Rings or (c) CB and P Rings, the Last of Which Supports a Wider Range of Substrates, e.g., Propargylammonium with 2-Azidoethylpyridinium to 5-Azidopentylpyridinium Salts



(β -CD) or γ -cyclodextrin (γ -CD), resulting in rapid and quantitative formation of [4]rotaxanes and higher oligorotaxanes. Hydrogen bonding between the rims of two CB rings and a CD torus gives rise to positive cooperativity²⁵ in the multicomponent assembly, boosting the rate of the CD–CB-AAC (Scheme 1a) on account of the ensemble's greatly

enhanced binding affinity for functionalized secondary dialkylammonium guests. Based on these initial findings, we envisaged that the observed positive cooperativity need not be restricted to CDs; other macrocycles, which are capable of multivalent (also bifurcated) hydrogen bonding and are complementary in shape or size to CB, might also aid and abet the efficient synthesis of oligorotaxanes.

Here, we report that the alkyne–azide 1,3-dipolar cycloaddition (AAC) templated by cucurbit[6]uril (CB), call it (Scheme 1b) the P–CB-AAC reaction, is also promoted by pillararenes,²⁶ a family of macrocycles composed of 5–10 hydroquinone rings linked through their para-positions by methylene bridges, as well as discovering that this combination of macrocycles is more accommodating to cationic substrates of different lengths, e.g., from 2- to 5-azidopentylbipyridinium units. It transpires that pillar[5]arene (P) alleviates the strict conformational preference of the P–CB-AAC reaction by stabilizing the geometry in which the positively charged bipyridinium (BIPY^{2+}) units move away from the portals of the CB, acting^{27,28} as a “molecular gasket”. In the same manner as a cofactor may be necessary to stabilize the catalytically active geometry of an enzyme, P modifies the binding properties of CB such that it will template the cycloaddition of substrates which are unreactive in the presence of CB alone. When the substrate length is increased, then two P gaskets bridge the longer gaps between CB rings, allowing both P-containing [4]- and [5]rotaxanes to be obtained in high yields. The four possible conformational isomers of the P rings that result from steric hindrance of the oxygen-through-the-annulus rotation of the hydroquinone rings are trapped as mixtures on the dumbbell components of these rotaxanes.

2. RESULTS AND DISCUSSION

In order to harness the positive cooperativity^{24,25} observed in our preliminary investigations²³ on oligo- and polyrotaxanes incorporating CB and CDs, it is useful to have a good understanding of the distribution of charge on the rims of these two rings. Examination of the calculated electrostatic potential map of CB reveals that the carbonyl oxygen atoms which adorn the periphery (Figure 1a) support high electron densities. The

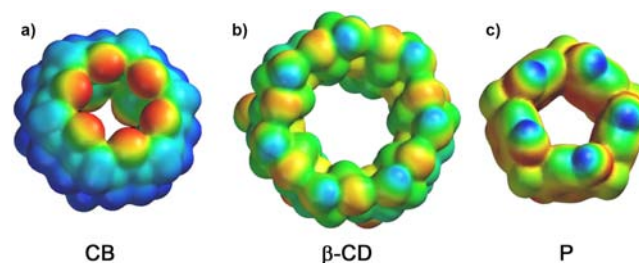
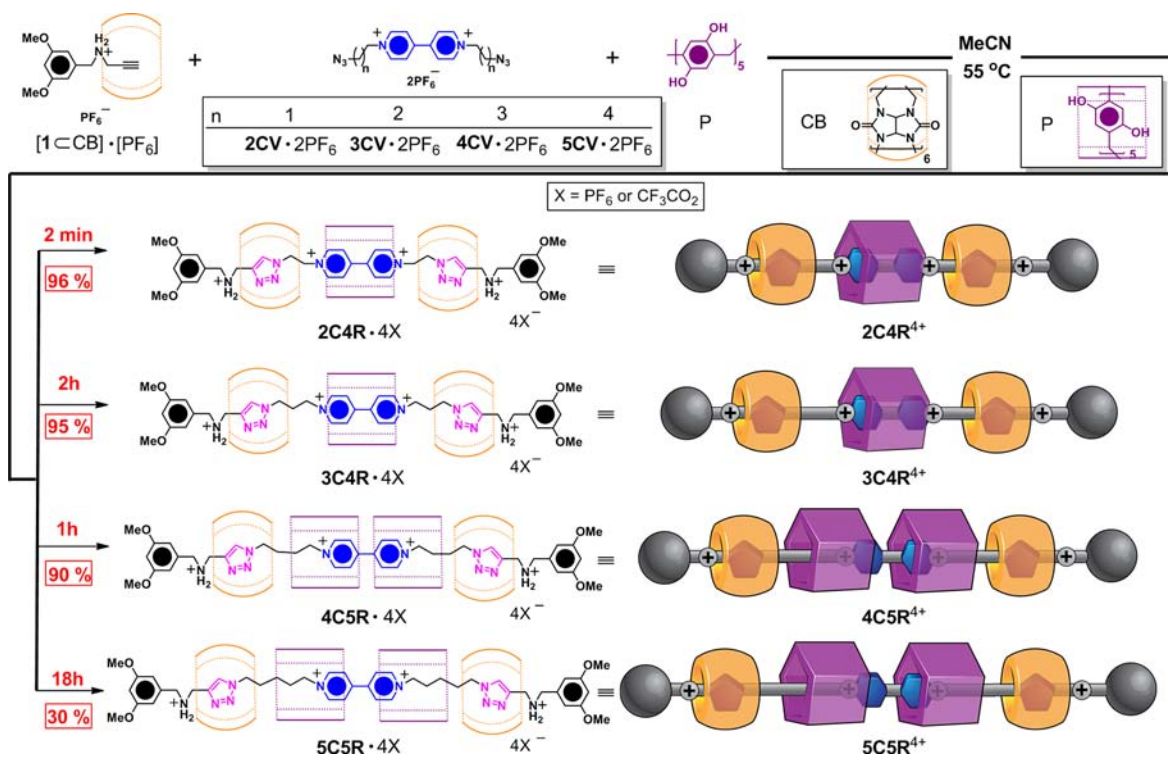


Figure 1. Electrostatic potential maps of (a) a CB ring, (b) a β -CD (secondary face) ring, and (c) a P ring, revealing the carbonyl oxygens (negatively charged, red) of the CB and the hydroxyl groups on each rim of the β -CD and P (positively charged, in blue) rings.

hydroxyl groups encircling the rims of β -CD (Figure 1b) are complementary, bearing as they do weak positive charges capable of acting as hydrogen bond donors. Although the rims of CB and β -CD are not matched in size, we discovered in our previous investigations²³ that β -CD still forms sufficiently strong hydrogen-bonding networks with two CB rings to favor [4]rotaxane formation. P presents an array of five phenolic

Scheme 2. Synthesis of the Hetero[4]rotaxanes $2C4R \cdot 4PF_6$ and $3C4R \cdot 4PF_6$ and the Hetero[5]rotaxanes $4C5R \cdot 4PF_6$ and $5C5R \cdot 4PF_6$, Starting from $[1CB] \cdot [PF_6]$, P, and the Viologen Derivatives ($2CV-5CV \cdot 2PF_6$), Respectively



hydroxyl groups on each face; analysis of their electrostatic potential map (Figure 1c) confirms that the hydroxyl groups on these macrocycles are more polarized than the hydroxyl groups on β -CD (Figure 1b), suggesting that they should take part in stronger hydrogen bonding interactions²⁹ with CB. In addition, P is the most easily accessible and thermodynamically stable pillararene homologue. While it does not commute perfectly with the 6-fold symmetry of CB, P is highly complementary in terms of rim size. For these reasons, it appeared to be a promising candidate to enhance the CB-AAC.³⁰ Accordingly, P was selected for further investigation of the cooperative capture process during the synthesis of oligorotaxanes.

Synthesis of Hetero[n]rotaxanes. On account of the different solubility profiles for CB and P, we were unable to find a solvent combination to dissolve both rings simultaneously: although CB can be induced into an aqueous solution in the presence of cations, P is insoluble in water. The problem was overcome by performing the organic-soluble alkyne-CB precursor by an “inclusion-followed-by-precipitation” process.³¹ A 1:1 mixture of *N*-(3,5-dimethoxybenzyl)propargylammonium chloride (1-Cl) with CB in aqueous solution was treated with NH_4PF_6 to afford the ternary complex $[1_2CB] \cdot [PF_6]_2$, which was isolated by filtration.³² Alternatively, the use of KPF_6 as the counterion-exchange reagent furnished the 1:1 complex $[1CB] \cdot [PF_6]$ because of the weaker CB–potassium compared to CB–ammonium interaction.³³ See the Supporting Information for details. These organic soluble complexes can then be employed as a convenient source of CB and the alkyne precursors.³⁴

When contemplating the use of P in the cooperative capture strategy, we posited that cationic BIPY²⁺ derivatives $CV \cdot 2PF_6$ (Scheme 2), which are known^{26a,35} to have a strong binding affinity for P in polar organic solvents (e.g., Me_2CO , MeCN, Me_2SO) would be more appropriate guests than previously

employed azidoalkylammonium salts.³⁶ As far as we are aware, BIPY²⁺ salts³⁷ have not been used in the CB-AAC process. A test reaction of $[1CB] \cdot [PF_6]$ with $2CV \cdot 2PF_6$ in MeCN afforded the [3]rotaxane $2C3R \cdot 4PF_6$ in an isolated yield of 30% and confirms the fact that BIPY²⁺ salts are viable substrates. See the Supporting Information for full details. The reaction was sluggish, however, and failed to reach completion, even after 2 days at 55 °C.

An initial trial of the P–CB-AAC (Scheme 1b) was conducted by mixing the rodlike precursor $2CV \cdot 2PF_6$ (1.0 equiv) and P (1.2 equiv) in MeCN before addition of the CB–alkyne complex $[1_2CB] \cdot [PF_6]_2$ (2.2 equiv), which was followed by a change in color of the reaction mixture from pale yellow to orange. Pleasingly, P brought about a considerable acceleration in the reaction rate and was incorporated into the product $2C4R \cdot 4PF_6$, confirming our hypothesis that it can take part in the cooperative capture of rotaxanes. In three parallel experiments, carried out at different temperatures and monitored by TLC, the reaction reached completion within 2 min (55 °C), 40 min (20 °C) and 2 h (–10 °C), respectively. The [4]rotaxane $2C4R \cdot 4PF_6$ was isolated (Table 1, entry 1, $[1_2CB]$) by column chromatography in 60–70% yield. Although satisfactory, the yield was somewhat lower than the cooperative capture mediated by CDs, which affords²³ [4]rotaxanes in up to 97%. The lower than expected yield may be attributed to competitive binding of the excess of the propargylammonium derivative present in the reaction mixture.³⁸ By simply substituting $[1_2CB] \cdot [PF_6]_2$ with the complex $[1CB] \cdot [PF_6]$, which has the desired 1:1 CB–alkyne stoichiometry, the efficiency of the reaction was improved: all starting materials were consumed, and ¹H NMR spectroscopic analysis of the crude reaction mixture indicated quantitative conversion to $2C4R \cdot 4PF_6$. The isolated yield (Table 1, entry 1, $[1CB]$) after column chromatography

Table 1. Isolated Yields of [4]/[5]Rotaxanes 2C4R-5C5R-4PF₆ Synthesized by Stopper Precursors [1CCB]·[PF₆]⁻ and [1₂CCB]·[PF₆]₂⁻ in Various Different Solvents

entry	rotaxanes	solvents	isolated yields (%)	
			[1CCB]·[PF ₆] ⁻	[1 ₂ CCB]·[PF ₆] ₂ ⁻
1	2C4R-4PF ₆	MeCN	96	70
2		Me ₂ CO	30 ^a	30 ^a
3		MeNO ₂	<5 ^a	<5 ^a
4		Me ₂ SO	NI ^{a,c}	NI ^{a,c}
5	3C4R-4PF ₆	MeCN	95	57
6		Me ₂ SO	NI ^{a,c}	NI ^{a,c}
7	4C5R-4PF ₆	MeCN	90	59
8		Me ₂ SO	NI ^{b,c}	NI ^{b,c}
9	5C5R-4PF ₆	MeCN	30	13
10		Me ₂ SO	NI ^{b,c}	NI ^{b,c}

^aConditions: [1CCB]·[PF₆]⁻ (or [1₂CCB]·[PF₆]₂⁻, 2.5 equiv), 2CV-2PF₆ (or 3CV-2PF₆, 1.0 equiv) and P (1.2 equiv), 55 °C, 48 h.

^bConditions: [1CCB]·[PF₆]⁻ (or [1₂CCB]·[PF₆]₂⁻, 2.5 equiv), 2CV-2PF₆ (or 3CV-2PF₆, 1.0 equiv) and P (2.2 equiv), 55 °C, 48 h. ^cNI = not isolated by silica gel chromatography.

was 96%, indicating that the P–CB–AAC is as efficient as the CD–CB–AAC. It is worth noting that, in CD₃CN at room temperature, the stopper precursor [1CCB]·[PF₆]⁻ disproportionates (Figure 2) overnight to afford the 2:1 complex [1₂CCB]·[PF₆]₂⁻ and CB. This process is driven by the precipitation of CB from solution, pushing the equilibrium toward [1₂CCB]·[PF₆]₂⁻.

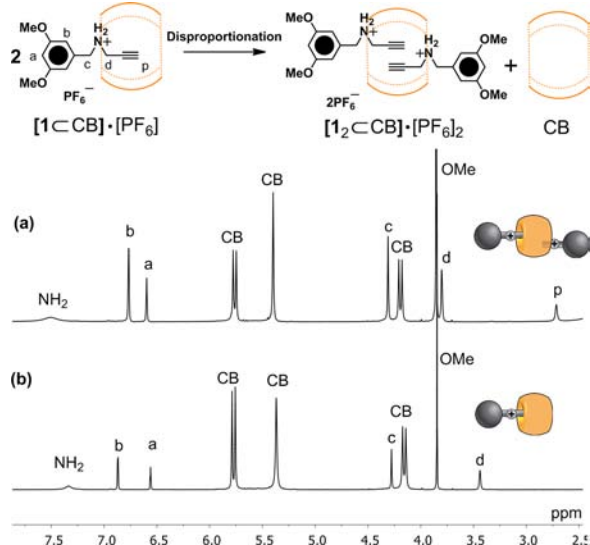


Figure 2. ¹H NMR spectra (500 MHz) of the stopper precursors (a) [1₂CCB]·[PF₆]₂⁻ and (b) [1CCB]·[PF₆]⁻ recorded in CD₃CN at 298 K.

Having established that the P–CB–AAC reaction tolerates an azidoethylbipyridinium substrate, and that the reaction is accelerated by P, we sought to explore BIPY²⁺ guests of different lengths. In the absence of P, no triazole ring products were formed after mixing stopper precursor [1CCB]·[PF₆]⁻ (or [1₂CCB]·[PF₆]₂⁻) with longer rod precursors 3CV-2PF₆ – 5CV-2PF₆ (Scheme 2). This observation is consistent with all previous reports^{14–16,37} that the distance between the alkyne/azide and the cation is critical for the supramolecular preorganization and, consequently, templated by CB. In the presence of P, however, the reaction of [1CCB]·[PF₆]⁻ with

3CV-2PF₆ in MeCN afforded (Table 1, entry 5, [1CCB]) the hetero[4]rotaxane 3C4R-4PF₆ (Scheme 2) in 95% isolated yield within 2 h at 55 °C. P apparently enables the CB–AAC, which does not take place in the presence of only CB or a CB–CD mixture,³⁹ by stabilizing an otherwise energetically unfavorable binding geometry of [1CCB]·[PF₆]⁻ and 3CV-2PF₆. This geometry allows the azide group at the end of the outstretched propylene chain to occupy the center of the CB cavity alongside the alkyne and thus undergo cyclization. Tentatively, we suggest that the ring component of an initial 3CV²⁺CP is relatively free to move along the vector of the BIPY²⁺ without paying a large energy penalty; that is, any increase in free energy as a result of translation is compensated for by the ring-to-ring hydrogen bonding network with CB upon quaternary complex formation. After installation of one triazole ring, the P moves to the other end of the BIPY²⁺ to stabilize the second P–CB–AAC reaction, installing the second stopper and forging the mechanical bond of the [4]rotaxane (Figure 3).

Upon lengthening the linear spacers yet further to butylene chains 4CV-2PF₆, no hetero[4]rotaxane was identified in the reaction containing stopper precursors, [1CCB]·[PF₆]⁻ and P. Instead, Mother Nature chooses (Scheme 2) a much more organized output, namely, a hetero[5]rotaxane 4C5R-4PF₆, which contains two P gaskets threaded onto the dumbbell. The [5]rotaxane 4C5R-4PF₆ was isolated (Table 1, entry 7, [1CCB]) in 90% yield after reaction of 4CV-2PF₆, [1CCB]·[PF₆]⁻ and P in 1:2.5:2.5 ratio at 20 °C for 1 h in MeCN solution. Decreasing the molar ratio of 4CV-2PF₆ and P (4CV²⁺:P = 1:1, 1:1.5, and 1:1.8) does not alter this outcome: no [3]- or [4]rotaxane was observed, and 4C5R-4PF₆ was the sole interlocked product. This observation implies that the two adjacent P rings^{35b,40} on the [5]rotaxane 4C5R-4PF₆ also communicate with each other through the inter-ring hydrogen bonding, leading to increased stability when compared to analogs with fewer rings and provides the lowest energy cycloaddition pathway.

The pentylene derivative 5CV-2PF₆ gave rise to hetero[5]rotaxane 5C5R-4PF₆, although the longer oligomethylene chain seems to impede the reaction, which requires 18 h to reach completion, resulting (Table 1, entry 9, [1CCB]) in a substantially reduced isolated yield of 30%. The decreased reaction rate, and the observation of the corresponding half-reacted dumbbell 5HD-3PF₆ and mono-P-[4]rotaxane analog (5C4R-4PF₆, see the Supporting Information for details) as minor products, suggest that the positive cooperativity has been curtailed, presumably because the four rings can no longer bridge the length of the fully extended dumbbell effectively. These results are consistent with a stepwise mechanism for the formation (Figure 3) of the [5]rotaxane 5C5R-4PF₆: after the first P–CB–AAC to introduce a stopper at one end of the dumbbell (i) the P ring may shuttle along the BIPY²⁺ subunit of the dumbbell to mediate the second P–CB–AAC and capture the [4]rotaxane 5C4R-4PF₆, (ii) the second P–CB–AAC can occur via an intermediate with two P gaskets encircling the dumbbell, giving rise to the [5]rotaxane 5C5R-4PF₆ with a hydrogen bond network that spans all four rings, or (iii) if no further reaction occurs, the pseudorotaxane intermediate dissociates during purification to yield the half dumbbell 5HD-3PF₆.

In keeping with these observations, the limit of this transformation was reached with the hexylene derivative

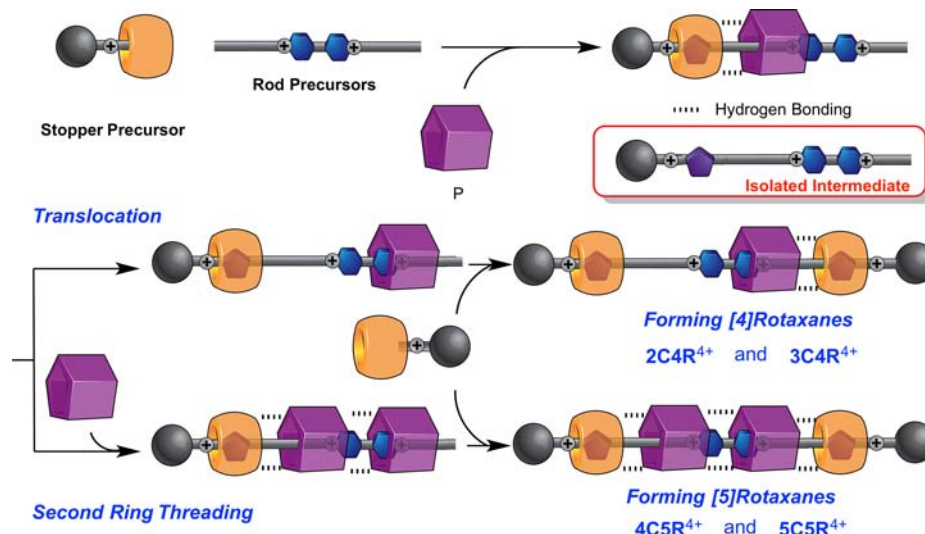


Figure 3. Graphical representation of the proposed mechanism for the formation of hetero[4]/[5]rotaxanes. The hatched lines in the graphical representation indicate the hydrogen bonding interactions between the CB and P rings.

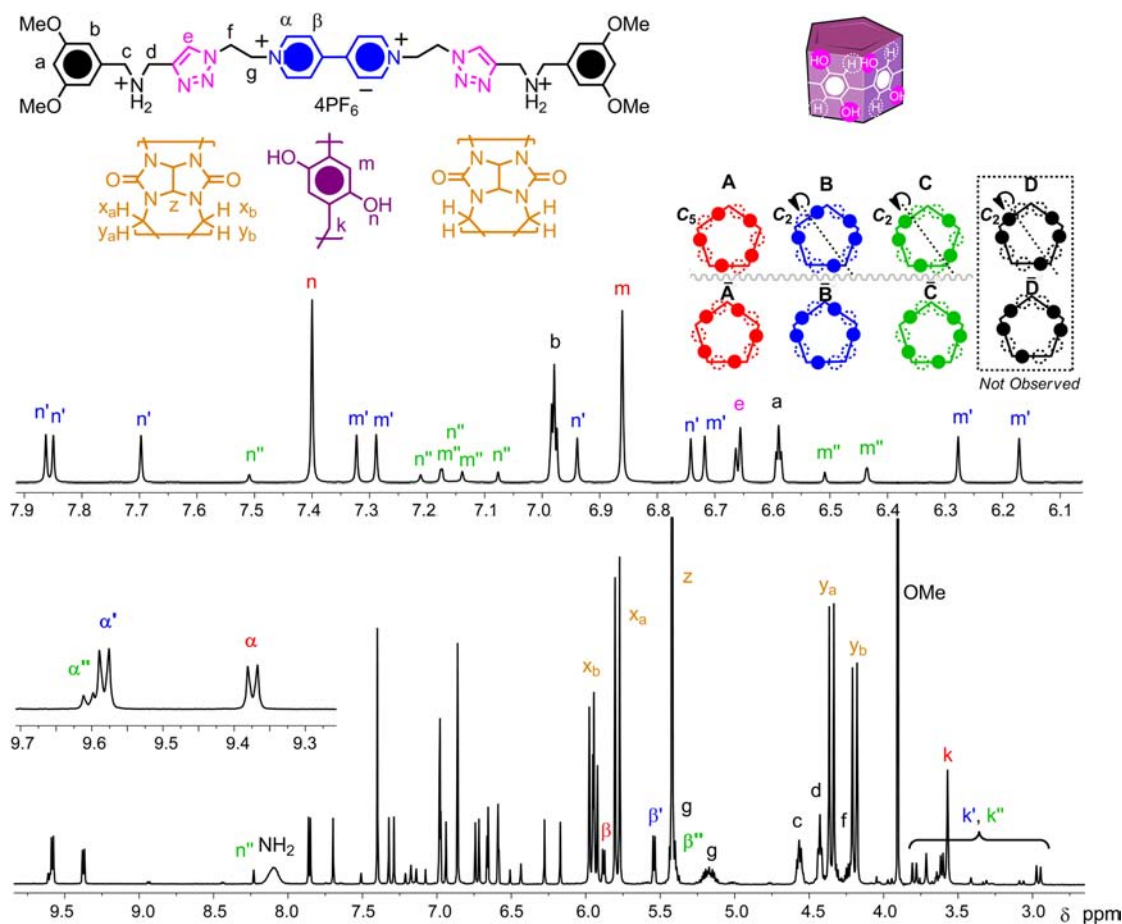


Figure 4. ^1H NMR spectrum (500 MHz) of $2\text{C}4\text{R}\cdot 4\text{PF}_6$, recorded in CD_3CN at 298 K. Three conformational isomers of the [4]rotaxane are present, colored in red ($2\text{C}4\text{R}_A\cdot 4\text{PF}_6$), blue ($2\text{C}4\text{R}_B\cdot 4\text{PF}_6$), and green ($2\text{C}4\text{R}_C\cdot 4\text{PF}_6$), respectively.

$6\text{CV}\cdot 2\text{PF}_6$ which only affords trace amounts of the [5]rotaxane $6\text{C}5\text{R}\cdot 4\text{PF}_6$ after stirring at 55°C for more than a week.

Solvent Effects. Initially, we probed the P–CB–AAC in MeCN as it appeared to be the most convenient solvent in which to dissolve the CB-containing precursors $[\text{1CCB}]\cdot[\text{PF}_6]$ and $[\text{1}_2\text{CCB}]\cdot[\text{PF}_6]_2$. During the course of our investigations,

we observed that the CV^{2+}CP , which is soluble in MeCN at the outset, gradually precipitates out of solution over a period of time (30 min to 1 h). This process appears to have little impact on reactions which proceed to completion within this time period, as evidenced by the excellent isolated yields; we suspect, however, that the lower yields, obtained over longer experiment

times, might be attributed in part to this process which effectively shuts down the reaction. Measuring the thermodynamic parameters for binding (binding constants K_a , enthalpy ΔH and entropy ΔS) of the P and (2-5CV)·2PF₆ complexes in MeCN, however, is not a trivial matter because of solubility issues. Switching to other polar solvents, e.g., MeNO₂ or Me₂CO, avoids the CV²⁺·CP solubility issue but raises new problems: when the rotaxation is performed in MeNO₂ or Me₂CO it requires (Table 1, entries 2 and 3) much longer reaction times (more than 18 h) with significantly lower yields (<50%) because of the poor solubility of the stopper precursors [1₂CCB]·[PF₆]₂ and [1₁CCB]·[PF₆].

P is known to form both 1:1 and 1:2 complexes with BIPY²⁺ derivatives in Me₂SO solutions:^{35b} indeed, a homogeneous solution of all reactants, including CV²⁺, P, and [1₂CCB]/[1₁CCB], can be achieved. Despite this practical breakthrough, no mechanically interlocked product was obtained (Table 1, entries 4, 6, 8, and 10) in the reaction. It seems that solvent–solute interactions dominate in Me₂SO because of its strong hydrogen bond acceptor capacity²⁹ ($\beta_{\text{sulfoxide}} = 8.9$, cf. $\beta_{\text{nitrile}} = 4.7$) which inhibits assembly of the productive multicomponent complexes. This result implies that the inter-ring hydrogen bonding interactions between CB, P and the substrates is the dominating factor in the P–CB–AAC.

Conformational Analysis. In principle, P can adopt (Figure 4) four enantiomeric pairs of diastereoisomeric conformations in solution on account of the oxygen-through-the-annulus rotation⁴¹ of the hydroquinone rings in P. These conformations undergo rapid inversion and interconversion in solution on the ¹H NMR time scale at room temperature. The rate of this rotation can be slowed down at low temperature (below –60 °C) in the presence of a BIPY²⁺ unit as a guest.⁴² Following the formation of 2C4R·4PF₆, the change in conformation of the P ring is impeded since its cavity is occupied by the BIPY²⁺ unit in the dumbbell, such that there is no space available for any of the hydroquinone rings to rotate through the annulus of P. For this reason, the hetero[4]-rotaxane 2C4R·4PF₆ can exist as four conformational isomers:⁴² A, B, C, and D with their corresponding enantiomers (Figure 4) \bar{A} , \bar{B} , \bar{C} , and \bar{D} . Conformational isomer A has C₃ symmetry, while the other three conformational isomers (B, C, and D) all have C₂ symmetry. Proton resonances (aromatic protons *m* and hydroxyl protons *n*, Figure 4) of P in conformational isomer A should exhibit two individual singlet peaks, while in the other three conformational isomers (B, C, and D) five singlet peaks for *m* and five singlet peaks for *n* should be exhibited, respectively, in the ¹H NMR spectrum.

The hetero[4]rotaxane 2C4R·4PF₆ was purified by column chromatography (SiO₂), and its formation was confirmed by the appearance of the resonance at 6.7 ppm for the triazole ring proton H_c in the ¹H NMR spectrum (Figure 4). Three sets of α proton resonances (δ 9.3–9.6 ppm in Figure 4) from the BIPY²⁺ unit in the dumbbell and three β proton resonances (δ 5.3–6.0 ppm) reveal the presence of three isomers associated with different P ring conformations. The β proton resonances are moved upfield compared with those for the rod precursor 2CV·2PF₆, while the α proton resonances are shifted significantly downfield, indicating that the β protons are shielded by P while the α protons are deshielded. This observation is consistent with the fact that the P ring encircles the BIPY²⁺ unit. On heating the hetero[4]rotaxane to 60 °C in CD₃CN and 100 °C in (CD₃)₂SO, we noted that the multiple

α and β proton resonances do not undergo coalescence on the ¹H NMR time scale. In the HSQC spectrum (see the Supporting Information), a total of 22 different OH and aromatic proton resonances (δ 6.1–8.3 ppm) can be observed (Figure 4) and assigned to the P ring. These observations suggest that the P ring of the hetero[4]rotaxane 2C4R·4PF₆ exists in three different conformations,⁴³ which are unable⁴⁴ to undergo inversion or interconversion upon heating to 100 °C.

Conformational isomer A (in red, Figure 4) of the P ring in 2C4R·4PF₆, which gives rise to the simplest spectrum on account of its C₃ symmetry, was identified first of all in the ¹H NMR spectrum, with the aid of two-dimensional NMR techniques (see the Supporting Information for the COSY, NOESY, HSQC, and HMBC NMR spectra). Identification of the other two conformational isomers out of the total three is not trivial: we begin with distinguishing proton *m* from *n* by HSQC and HMBC spectra, followed by linking the all-neighboring protons sequentially in the same P ring by 2D NOESY experiments. 2D NOESY spectra of 2C4R·4PF₆ have been obtained with different mixing times (200 ms, 300 ms, and 400 ms, respectively) at 298 K. A full build-up NOE signal between protons *m* and *n* on the P rings requires a longer mixing time (≥ 400 ms). On the basis of an analysis of the NOE correlation peaks (see the Supporting Information), two conformational isomers, namely, B (in blue) and C (in green), can be identified in the ¹H NMR spectrum (Figure 4): conformational isomer D is not observed. The populations of the conformational isomers in 2C4R·4PF₆, calculated from integration of their particular ¹H NMR signals, are (Table 2) in

Table 2. Conformational Isomer Distribution of the [4]Rotaxanes 2C4R·4PF₆ and 3C4R·4PF₆ Synthesized in MeCN at Different Temperatures

[4]rotaxane	temp (°C)	conformational isomer distribution ^a (%)			
		A + \bar{A}	B + \bar{B}	C + \bar{C}	D + \bar{D}
2C4R·4PF ₆	–10	36	52	12	NO ^b
	25	29	55	16	NO
	55	17	59	24	NO
3C4R·4PF ₆	55	30	40	23	7

^athe conformational isomer distribution was calculated from the relative integrated intensities of proton resonances for each conformational isomer of the hetero[4]-, [5]rotaxanes in the ¹H NMR spectra. ^bNO = not observed.

the sequence of B > A > C. In order to acquire a better understanding of the conformational composition, 2C4R·4PF₆ was synthesized at –10 and 55 °C, respectively. The kinetics of the rotaxane formation are significantly different at these temperatures; i.e., the reaction goes to completion within 2 min at 55 °C but requires 2 h to do so at –10 °C. Once again, only three conformational isomers (A, B and C) are observed in the ¹H NMR spectra. When the temperature of the reaction is low, only the population of conformational isomer A increases gradually, an observation indicates that 2C4R_(A/ \bar{A}) is the thermodynamically most favorable product. Conformational isomer A, which supports the least number of intraring hydrogen bonds (OH–OH hydrogen bonding) in the P ring, is able to form the strongest hydrogen bonding network with CBs on the dumbbell of 2C4R·4PF₆. By contrast, the OH groups in conformational isomer D which has the greatest propensity to form intraring hydrogen bonds⁴³ are less able to form hydrogen bonds with CB. Even when the reaction is

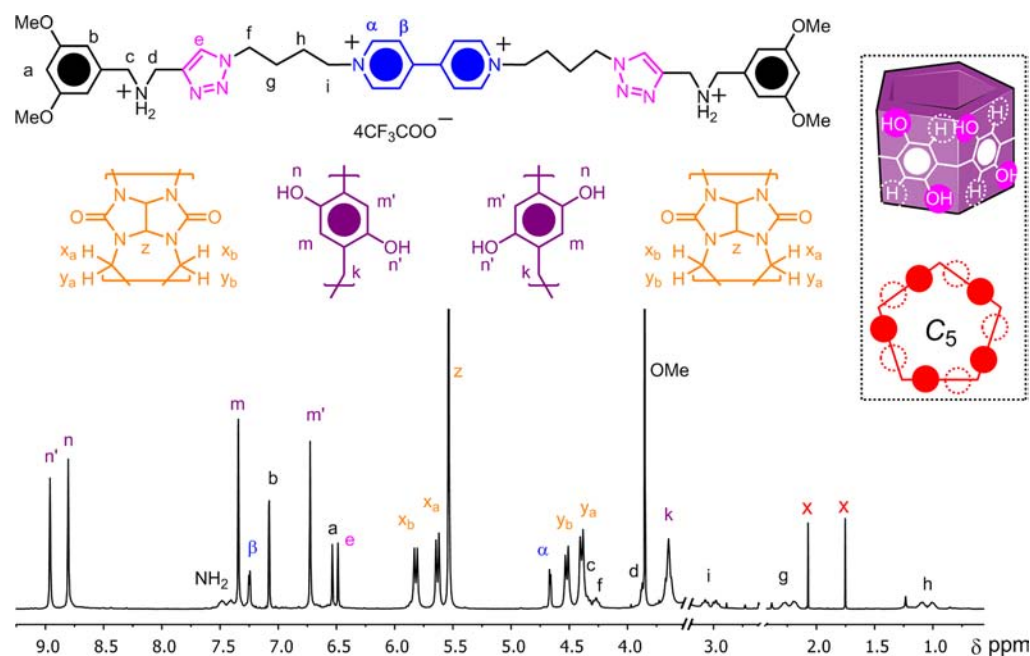


Figure 5. ^1H NMR spectrum (600 MHz) of $4\text{C5R}_{\text{AA}}\cdot 4\text{TFA}$, recorded in $(\text{CD}_3)_2\text{SO}$ at 298 K.

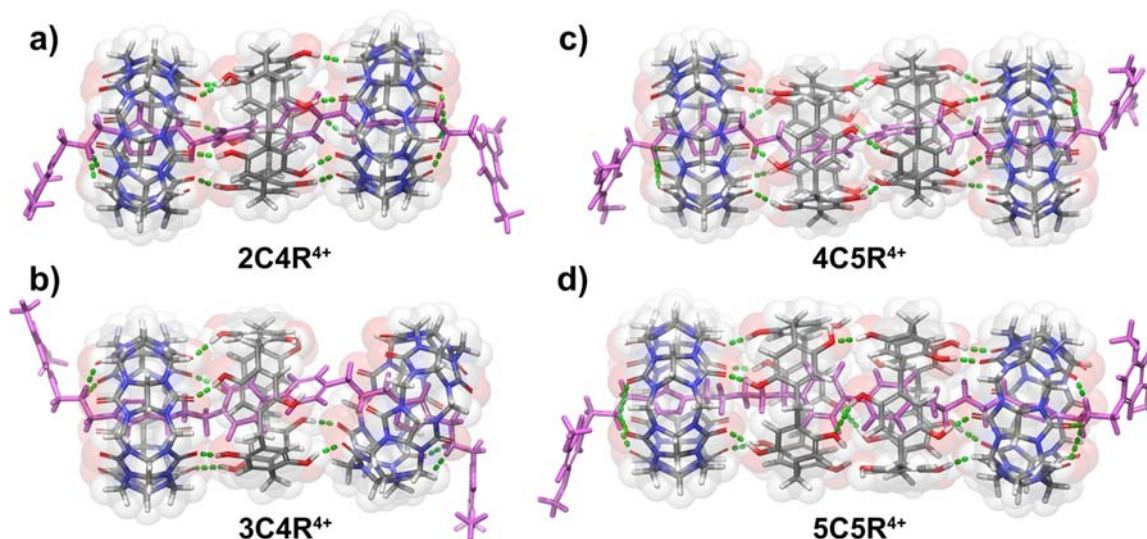


Figure 6. Computationally generated structure of the hetero[n]rotaxanes (a) 2C4R^{4+} , (b) 3C4R^{4+} , (c) 4C5R^{4+} , and (d) 5C5R^{4+} using a simulated annealing process employing the OPLS-2005 force field, in which all P rings adopt conformation A with C_5 symmetry as shown in Figure 4. The green dashed lines indicate the hydrogen-bonding interactions in these rotaxanes.

performed at $-10\text{ }^\circ\text{C}$, the major product is $2\text{C4R}_{(\text{B}/\bar{\text{B}})}$, an observation which suggests that the energy difference between conformational isomers A and B is really quite small.

Four conformational isomers (A, B, C, and D) can be observed in the ^1H NMR spectrum of the hetero[4]rotaxane $3\text{C4R}\cdot 4\text{PF}_6$. By following a procedure similar to that adopted for $2\text{C4R}\cdot 4\text{PF}_6$, all the conformational isomers could be identified and their relative populations were found to be A (30%), B (40%), C (23%), and D (7%), respectively. This observation suggests that all four conformational isomers of P can form stable complexes with $3\text{CV}\cdot 2\text{PF}_6$ in solution and hence be captured by the rod precursor $[\text{1CCB}]\cdot [\text{PF}_6]$. The relative populations of the conformational isomers of P in $3\text{C4R}\cdot 4\text{PF}_6$ follow a similar trend to those of P in $2\text{C4R}\cdot 4\text{PF}_6$. The α and β protons of the BIPY^{2+} unit in $3\text{C4R}\cdot 4\text{PF}_6$ are less

shielded and deshielded by P, respectively, than in $2\text{C4R}\cdot 4\text{PF}_6$. This comparison implies that the P ring can shuttle along the BIPY^{2+} unit in $3\text{C4R}\cdot 4\text{PF}_6$ because of its extended oligomethylene chain length. In addition, even although the P ring adopts the same conformations in $3\text{C4R}\cdot 4\text{PF}_6$, the chemical shifts of resonances for protons signals m and n in the conformational isomers A, B and C are very different compared with those in the corresponding conformational isomers in $2\text{C4R}\cdot 4\text{PF}_6$.

In theory, the hetero[5]rotaxane $4\text{C5R}\cdot 4\text{PF}_6$ bearing two P rings on its dumbbell can exist (see the Supporting Information) as 20 different stereoisomers. The proton signals in the ^1H NMR spectrum of $4\text{C5R}\cdot 4\text{PF}_6$ are not well separated, rendering the full analysis of the each P conformation extremely challenging. Fortunately, the most abundant conformation

present in **4C5R**-4PF₆ can be separated by recycling reverse phase HPLC. There are two hydroxyl protons signals at 9.0 ppm as well as two aromatic protons (7.35 and 6.73 ppm) which can be assigned (Figure 5) to P. This assignment indicates that in this fraction, the two P rings adopt conformation A/ \bar{A} with C₅ symmetry, obligating one set of protons (*n* and *m*) to point toward the CB ring and another set (*n'* and *m'*) to point away. There are still, however two enantiomers (AA and $\bar{A}\bar{A}$) and one other stereoisomer (A \bar{A}). It is worth noting that the resonance (δ = 4.67 ppm) for the α proton in the BIPY²⁺ unit is shifted upfield significantly whereas the resonance for the β proton is shifted downfield. In addition, the resonances for protons *g* and *h* of the oligomethylene chain are shielded and their resonances appear at high field compared to those for the rod precursor. This phenomenon suggests that two P rings are threaded along the dumbbell symmetrically, each of them occupying half of the BIPY²⁺ unit and the oligomethylene chain. The formation of a highly symmetrical structure in the case of **4C5R** is under thermodynamic control. The P ring conformational preference in the hetero[5]rotaxane **4C5R** is a consequence of the relative strength of the hydrogen bonding interactions – whereas both the CB-P_A and CB-P_B inter-ring interactions are of similar energy, optimal hydrogen bonding between P rings only occurs when both adopt their C₅ conformations.

Molecular Modeling. Slow vapor diffusion of *i*Pr₂O into a MeNO₂ solution of rotaxane **2C4R** afforded single crystals suitable for X-ray diffraction. Alas, the crystals were weakly diffracting and the data could be refined to a resolution of 1.30 Å (see the Supporting Information): the situation is, no doubt, complicated by the presence of isomers giving rise to disorder in the solid state. From the partially resolved structure, it is possible to distinguish the three ring components threaded on the dumbbell, with a P ring positioned between two CB rings. Since no detailed structural information could be garnered from this data, we appealed to molecular mechanics simulations in order to gain a better understanding of the noncovalent bonding interactions that direct rotaxane formation and influence the choice and close up distribution of isomers. Simulations were performed starting from all four P isomers (A–D in Figure 4) to determine the lowest energy structure for the rotaxane **2C4R**: see the Supporting Information. The simulated structure (Figure 6a) of **2C4R** incorporating a P ring locked in conformation A closely matches the structure suggested by the X-ray crystallographic analysis.⁴⁶ Owing to its C₅ symmetric conformation, all phenolic hydroxyl groups in this conformation of P are able to participate in hydrogen bonding interactions with the neighboring carbonyl groups of the CBs, thus maximizing the stabilizing inter-ring interactions. The capacity of P ring in its C₅ symmetric conformation to participate in inter-ring hydrogen bonding is diminished in the case of the C₂ symmetric conformations B–D as a result of internal hydrogen bonding between some of the phenolic hydroxyl groups. The P ring of the rotaxane **2C4R** in conformation D was found to have the maximized intraring hydrogen bonding, in keeping with the fact that it has the fewest inter-ring hydrogen bonding interactions with CB rings. This difference in the inter-ring hydrogen bonding networks may explain why conformational isomer D was not observed for **2C4R** in practice.

We have discovered that lengthening the rod precursor by two methylene units slows down rotaxane formation from 2 min (**2C4R**) to 2 h (**3C4R**). It is evident from the simulated

structure of **3C4R** that the contiguous hydrogen bonding network is disrupted, with fewer inter-ring hydrogen bonds. The CB rings, which occupy the ammonium binding sites, are held much further apart, preventing the P ring from sealing the gap between them completely. During formation of **3C4R**, the ensemble benefits much less from the positive cooperativity, generated by inter-ring hydrogen bonding, leading to a reduced reaction rate. Additionally, the energy difference between isomers of **3C4R** is not as significant as it is in the case of **2C4R**, in accordance with the fact that all four isomers have been identified experimentally on the dumbbell of **3C4R**.

[5]Rotaxanes **4C5R** and **5C5R** follow a similar trend to those of the [4]rotaxanes **2C4R** and **3C4R**. The spacing of rings (Figure 6c) in **4C5R** is optimal, leading to (i) a high degree of positive cooperativity, (ii) a high yield, (iii) a short reaction time, and (iv) a noticeable preference for the isomers (**4C5R**_{AA}, **4C5R**_{A \bar{A}} and **4C5R** _{$\bar{A}\bar{A}$}) in which the P rings adopt C₅ conformation. The longer oligomethylene chains in **5C5R** (Figure 6d) result in longer inter-ring hydrogen bonding distances and, hence, weaker interactions. A consequence of changing the strength of the inter-ring interactions is reflected in a change in the specificity of the reaction favoring the [5]rotaxane, i.e., **4C5R** is preferred over the [5]rotaxanes regardless of the reaction stoichiometry, but the [4]rotaxane analog (**5C4R**) of the [5]rotaxane **5C5R** was identified as a side product.

CONCLUSIONS

The cooperative capture strategy²³ for templating the formation of heterorotaxanes containing cyclodextrins has been extended to the use of pillar[5]arene rings as promoters. Compared to the interactions between cyclodextrins and cucurbiturils, the superior hydrogen-bonding interactions between the faces of cucurbit[6]uril and pillar[5]arene, provided the constitutions of the dumbbells are of appropriate lengths, can (i) accelerate 1,3-dipolar cycloadditions between azides and alkynes, affording two three-ring rotaxanes and one four-ring rotaxane in high yields, as well as (ii) support cycloadditions with a broader range of substrates, varying from 2-azidoethyl- to 5-azidopentylpyridinium ions. The siting of the pillar[5]arene rings around bipyridinium units stabilizes otherwise energetically unfavorable coconformations of the alkyne and azide moieties within the cucurbit[6]uril cavity, and allows pillar[5]arene ring(s) to promote cycloadditions at each end of the nascent dumbbells sequentially. All four conformations (A–D) of pillar[5]arene have been observed experimentally and characterized fully by ¹H NMR spectroscopy in the case of **3C4R**. The populations of the trapped and fixed conformational isomers⁴² of the pillar[5]arenes in the hetero[4]/[5]rotaxanes appear to be at least partially under thermodynamic control, while the relative yields of one (**2C4R**_A) of the isomers is observed to increase as the reaction temperature decreases. Molecular mechanical simulations also suggest that the relative energies among the conformational isomers in these rotaxanes are similar. The cooperative hydrogen-bonding interactions between cucurbit[6]uril and pillar[5]arene rings give rise to a high level of preorganization during rotaxane formation, which, on one hand, greatly enhances cucurbit[6]uril's activity toward templating the 1,3-dipolar cycloaddition and, on the other hand, controls the conformational distribution of the pillar[5]arene rings. These results add yet another cooperative approach to the syntheses of mechanically interlocked molecules with high efficiencies and good constitu-

tional integrities. Furthermore, a new strategy for altering template activity employing noncovalent bonding interactions has been demonstrated. These findings expand the use of cucurbituril-catalyzed 1,3-dipolar cycloadditions for the development of highly ordered polyrotaxanes and add a fresh approach to the practice of supramolecular catalysis.

EXPERIMENTAL SECTION

General Methods. All reagents were purchased from commercial suppliers (Aldrich and Fisher) and used as received. Pillar[5]arene^{26h} (P), cucurbit[6]uril⁴⁷ (CB), and the rod precursors⁴⁸ (2-6CV·2PF₆) were synthesized as reported in the literature. Thin-layer chromatography (TLC) was performed on silica gel 60 F254 (E. Merck). Column chromatography was carried out on silica gel 60F (Merck 9385, 0.040–0.063 mm). *Caution:* Significant amounts of rotaxanes 2C4R–5C5R·4PF₆ are retained on silica columns, and so it is important to use a minimum amount of silica gel. UV–vis Spectra were measured on a Shimadzu 3600 UV–vis–NIR spectrometer with a temperature control system, employing cuvettes with a pathway of either 2 or 10 mm. Nuclear magnetic resonance (NMR) spectra were recorded on Bruker Avance 500 or 600 spectrometers with working frequencies of 500 or 600 MHz for ¹H and 125 or 150 MHz for ¹³C nuclei, respectively. Chemical shifts are reported in ppm relative to the signals corresponding to the residual nondeuterated solvents (CDCl₃: δ = 7.26 ppm, CD₃CN: δ = 1.94 ppm, D₂O: δ = 4.62 ppm and (CD₃)₂SO: δ = 2.50 ppm). High-resolution mass spectra were measured on a Finnigan LCQ iontrap mass spectrometer (HR-ESI).

[1CCB]·[PF₆]. 1-Cl (600 mg, 2.5 mmol) and CB (2.5 g, 2.5 mmol) in H₂O (70 mL) were stirred at 90 °C for 1 h, after which time the reaction mixture was cooled down to room temperature and the insoluble residue removed by filtration. When KPF₆ (5.0 g, 27.1 mmol) was added to the aqueous solution, a white precipitate was generated. The solid was collected by filtration, washed with excess of H₂O and dried under reduced pressure to afford [1CCB]·[PF₆] (3.2 g, yield 95%): ¹H NMR (500 MHz, CD₃CN) δ = 7.34 (bs, 2H), 6.87 (d, J = 2.3 Hz, 2H), 6.56 (t, J = 2.2 Hz, 1H), 5.77 (d, J = 15.1 Hz, 12H), 5.37 (s, 12H), 4.28 (s, 2H), 4.16 (d, J = 15.2 Hz, 12H), 3.85 (s, 6H), 3.44 (s, 2H), 2.16 (s, 1H).

[I₂CCB]·[PF₆]₂. 1-Cl (200 mg, 0.83 mmol) and CB (800 mg, 0.80 mmol) in H₂O (50 mL) were stirred at 60 °C overnight, and the insoluble residue was removed by filtration. When NH₄PF₆ (1.62 g, 10 mmol) was added to the aqueous solution, a white precipitate was generated. The solid was collected by filtration, washed with excess of H₂O and dried under reduced pressure to afford [I₂CCB]·[PF₆]₂ (1.34 g, yield 95%): ¹H NMR (500 MHz, CD₃CN) δ = 6.80 (bs, 4H), 6.58 (t, J = 2.3 Hz, 2H), 5.76 (d, J = 15.2 Hz, 12H), 5.38 (s, 12H), 4.32 (s, 4H), 4.17 (d, J = 15.2 Hz, 12H), 3.84 (s, 12H), 3.70 (s, 4H); ¹³C NMR (126 MHz, CD₃CN) δ = 160.9, 155.3, 155.1, 132.3, 107.5, 100.7, 69.4, 68.2, 54.9, 50.8, 50.3, 49.6, 49.5, 35.4; HR-ESI-MS calcd for [M – 2PF₆]²⁺ m/z = 704.2647, found m/z = 704.2643; calcd for [M – PF₆]⁺ m/z = 1553.4941, found m/z = 1553.4897.

2C4R·4PF₆. (*Approach 1*) [1CCB]·[PF₆] (172 mg, 127.6 μmol), 2CV·2PF₆ (25 mg, 42.6 μmol), and P (35 mg, 57.4 μmol) were dissolved in MeCN (30 mL) and the mixture stirred at room temperature. The color of the reaction mixture turns orange immediately. The reaction was monitored by TLC (SiO₂: Me₂CO with 2% NH₄PF₆ (m/v), I₂ stain, R_f = 0.3) and was found to be complete inside 1 h. The solvent was then removed under reduced pressure, and the residue was purified by column chromatography (SiO₂: Me₂CO with 0.2% NH₄PF₆ and then Me₂CO with 2% NH₄PF₆ (m/v)). The fraction with R_f = 0.3 (TLC/SiO₂: Me₂CO with 2% NH₄PF₆ (m/v)) was collected, and the solvent was removed under the reduced pressure. H₂O (20 mL) was added to the residue to remove excess of NH₄PF₆, and the product “crashed out” as an orange precipitate. The solid was collected by filtration, washed with an excess of H₂O to remove NH₄PF₆, and dried under high vacuum to afford the hetero[4]rotaxane 2C4R·4PF₆ as an orange powder (145 mg, yield 95%). (*Approach 2*) 2CV·2PF₆ (10 mg, 17.1 μmol) and P (16 mg, 26.2 μmol) were dissolved in MeCN (20 mL) and stirred at an appropriate

temperature (–10 °C, 25 and 55 °C, respectively) until complex formation reached equilibrium. Then, [I₂CCB]·[PF₆]₂ (65 mg, 38.3 μmol) was added in one portion to the reaction mixture, whereupon the color of the mixture changed to orange. The reaction was monitored by TLC (SiO₂: Me₂CO with 2% NH₄PF₆ (m/v), I₂ stain, R_f = 0.3). After all of the 2CV·2PF₆ had been consumed, the solvent was removed under reduced pressure and the residue was purified by column chromatography (SiO₂: Me₂CO with 0.2% NH₄PF₆ and then Me₂CO with 2% NH₄PF₆ (m/v)). The fraction with R_f = 0.3 (TLC/SiO₂: Me₂CO with 2% NH₄PF₆ (m/v)) was collected, and the solvent was removed under reduced pressure. H₂O (20 mL) was added to the residue to remove excess of NH₄PF₆, whereupon the product “crashed out” as an orange precipitate. The solid was collected by filtration, washed with an excess of H₂O to remove NH₄PF₆, and dried under high vacuum to afford the hetero[4]rotaxane 2C4R·4PF₆ as an orange powder (yield 60–70%).

In the ¹H NMR spectrum of hetero[4]rotaxane 2C4R·4PF₆, three, namely 2C4R_A·4PF₆, 2C4R_B·4PF₆ and 2C4R_C·4PF₆, of the four possible conformational isomers 2C4R_A·4PF₆, 2C4R_B·4PF₆, 2C4R_C·4PF₆ and 2C4R_D·4PF₆ were observed. No 2C4R_D·4PF₆ was detected by ¹H NMR spectroscopy. When the separation of the three conformational isomers was attempted using recycling reversed-phase HPLC, the isomers invariably eluted together as a mixture. HR-ESI-MS of the three-component mixture of 2C4R·4PF₆: calcd for [M – 4PF₆]⁴⁺ m/z = 827.7894, found m/z = 827.7890, [M – 3PF₆]³⁺ m/z = 1152.0406, found m/z = 1152.0403, [M – 3PF₆ – HPF₆]³⁺ m/z = 1103.3835, found m/z = 1103.3829. By comparing the relative integrated intensities for each of the proton resonances in the ¹H NMR spectrum with 2D ¹H–¹H COSY, ¹H–¹³C HSQC, and ¹H–¹H NOESY spectra (see the Supporting Information), we were able to assign every proton signal in the ¹H NMR spectrum to one of the three conformational isomers. The relative conformations (A, B and C) of the P rings were assigned by ¹H–¹H NOESY spectra and the relative abundances of the three isomers in the mixture obtained from integration are listed in Table 2. We have extracted the proton signal assignments for each conformational isomer (A, B and C) of 2C4R·4PF₆ and listed them below. Note that the proton counts listed below are relative ones for each conformational isomer.

Conformational isomer 2C4R_A·4PF₆: ¹H NMR (600 MHz, CD₃CN) δ 9.35 (d, J = 6.6 Hz, 4H), 8.07 (bs, 4H), 7.36 (s, 10H), 6.96 (m, 4H), 6.84 (s, 10H), 6.64 (s, 2H), 6.57 (t, J = 2.3 Hz, 2H), 5.93 (dd, J = 15.5, 12H), 5.86 (d, J = 6.7 Hz, 4H), 5.77 (d, J = 15.4 Hz, 12H), 5.40 (s, 24H), 5.21–5.10 (m, 4H), 4.54 (t, J = 6.0, 4H), 4.41 (t, J = 5.9 Hz, 4H), 4.32 (d, J = 15.5 Hz, 12H), 4.24–4.20 (m, 4H), 4.17 (d, J = 15.4, 12H), 3.88 (s, 12H), 3.55 (s, 10H). Conformational isomer 2C4R_B·4PF₆: ¹H NMR (600 MHz, CD₃CN) δ 9.57 (d, J = 6.5 Hz, 4H), 8.07 (bs, 4H), 7.82 (s, 2H), 7.81 (s, 2H), 7.65 (s, 2H), 7.30 (s, 2H), 7.26 (s, 2H), 6.96 (m, 4H), 6.91 (s, 2H), 6.71 (d, 2H), 6.70 (s, 2H), 6.64 (s, 2H), 6.57 (t, J = 2.3 Hz, 2H), 6.26 (s, 2H), 6.15 (s, 2H), 5.93 (dd, J = 15.5, 12H), 5.77 (d, J = 15.4 Hz, 12H), 5.52 (d, J = 6.7 Hz, 4H), 5.40 (s, 24H), 5.21–5.10 (m, 4H), 4.54 (t, J = 6.0, 4H), 4.41 (t, J = 5.9 Hz, 4H), 4.32 (d, J = 15.5 Hz, 12H), 4.24–4.20 (m, 4H), 4.17 (d, J = 15.4, 12H), 3.88 (s, 12H), 3.78 (d, J = 13.8 Hz, 2H), 3.69 (s, 2H), 3.57 (m, 4H), 2.94 (d, J = 13.9 Hz, 2H). Conformational isomer 2C4R_C·4PF₆: ¹H NMR (600 MHz, CD₃CN) δ 9.58 (d, J = 6.6 Hz, 4H), 8.18 (s, 2H), 8.07 (bs, 4H), 7.47 (s, 2H), 7.18 (s, 2H), 7.15 (s, 2H), 7.14 (s, 3H), 7.11 (s, 3H), 7.04 (s, 3H), 6.96 (m, 4H), 6.64 (s, 2H), 6.57 (t, J = 2.3 Hz, 2H), 6.49 (s, 2H), 6.42 (s, 2H), 6.41 (s, 2H), 5.93 (dd, J = 15.5, 12H), 5.77 (d, J = 15.4 Hz, 12H), 5.40 (s, 24H), 5.35 (d, J = 6.1 Hz, 4H), 5.21–5.10 (m, 4H), 4.54 (t, J = 6.0, 4H), 4.41 (t, J = 5.9 Hz, 4H), 4.32 (d, J = 15.5 Hz, 12H), 4.24–4.20 (m, 4H), 4.17 (d, J = 15.4, 12H), 3.94 (d, J = 13.7 Hz, 2H), 3.88 (s, 12H), 3.62 (m, 4H), 3.40 (s, 2H), 3.05 (d, J = 14.1 Hz, 2H).

3C4R·4PF₆. (*Approach 1*) [1CCB]·[PF₆] (172 mg, 127.6 μmol), 3CV·2PF₆ (25 mg, 40.7 μmol), and P (35 mg, 57.4 μmol) were dissolved in MeCN (30 mL) and the mixture stirred at 55 °C. The color of the reaction mixture turned orange immediately. The reaction was monitored by TLC (SiO₂: Me₂CO with 2.5% NH₄PF₆ (m/v), I₂ stain, R_f = 0.3) and was found to be complete inside 2 h. The solvent was removed under reduced pressure and the residue was purified by

column chromatography (SiO₂: Me₂CO with 0.2% NH₄PF₆ and then Me₂CO with 3% NH₄PF₆ (m/v)). The fraction with R_f = 0.3 (TLC/SiO₂: Me₂CO with 2.5% NH₄PF₆ (m/v)) was collected, and the solvent was removed under the reduced pressure. H₂O (20 mL) was added to the residue to remove excess of NH₄PF₆, whereupon the product "crashed out" as an orange precipitate. The solid was collected by filtration, washed with an excess of H₂O to remove NH₄PF₆ and dried under high vacuum to afford the hetero[4]rotaxane 3C4R·4PF₆ as an orange powder (145 mg, yield 95%). (Approach 2) 3CV·2PF₆ (12 mg, 18.7 μmol) and P (18 mg, 29.5 μmol) were dissolved in MeCN (20 mL) and stirred at 55 °C until complex formation reached equilibrium. Then, [1₂CCB][PF₆]₂ (65 mg, 38.3 μmol) was added in one portion to the reaction mixture, whereupon the color of the mixture changes to orange. The reaction was monitored by TLC (SiO₂: Me₂CO with 2.5% NH₄PF₆ (m/v), I₂ stain, R_f = 0.3). After all of the 2CV·2PF₆ had been consumed, the solvent was removed under reduced pressure and the residue was purified by column chromatography (SiO₂: Me₂CO with 0.2% NH₄PF₆ and then Me₂CO with 3% NH₄PF₆ (m/v)). The fraction with R_f = 0.3 (TLC/SiO₂: Me₂CO with 2.5% NH₄PF₆ (m/v)) was collected, and the solvent was removed under the reduced pressure. H₂O (20 mL) was added to the residue to remove excess of NH₄PF₆, whereupon the product "crashed out" as an orange precipitate. The solid was collected by filtration, washed with an excess of H₂O to remove NH₄PF₆, and dried under high vacuum to afford the hetero[4]rotaxane 3C4R·4PF₆ as an orange powder (yield 59%).

In the case of the hetero[4]rotaxane 3C4R·4PF₆, all four possible conformational isomers, namely 3C4R_A·4PF₆, 3C4R_B·4PF₆, 3C4R_C·4PF₆, and 3C4R_D·4PF₆ have been observed by ¹H NMR spectroscopy. When the separation of the four conformational isomers was attempted using recycling reverse phase HPLC, the isomers invariably eluted together as a mixture. HR-ESI-MS of the four-component mixture of 3C4R·4PF₆: calcd for [M - 4PF₆]⁴⁺ m/z = 834.7969, found m/z = 834.7972, [M - 3PF₆]³⁺ m/z = 1161.3841, found m/z = 1161.3833, [M - 3PF₆ - HPF₆]³⁺ m/z = 1112.7267, found m/z = 1112.7259. By comparing the relative integrated intensities for each of the proton resonances in the ¹H NMR spectrum with 2D ¹H-¹H COSY, ¹H-¹³C HSQC, and ¹H-¹H NOESY spectra (see the Supporting Information), we were able to assign every proton signal in the ¹H NMR spectrum to one of the four conformational isomers. The relative conformations (A, B, C and D) of the P rings were assigned from an analysis of the ¹H-¹H NOESY spectra and the relative abundances of the four isomers in the mixture are listed in Table 2. We have extracted the proton signal assignments for each conformational isomer (A, B, C and D) of 3C4R·4PF₆ and they are listed below. Note that the proton counts listed below are the relative ones for each conformational isomer.

Conformational isomer 3C4R_A·4PF₆: ¹H NMR (600 MHz, CD₃CN) δ 8.63 (d, J = 6.5 Hz, 4H, α), 8.16 (bs, 4H, NH₂), 7.38 (s, 10H, OH), 6.93 (m, 4H, b), 6.81 (s, 10H, ArH), 6.56 (m, 2H, a), 6.50 (s, 2H, e), 5.95–5.71 (m, 24H, x_a + x_b), 5.89 (d, J = 6.5 Hz, 4H, β), 5.33 (s, 24H, z), 4.80 (m, 4H, h), 4.44–4.39 (m, 8H, c and d), 4.24 (d, J = 15.2 Hz, 12H, y_b), 4.11 (d, J = 15.2 Hz, 12H, y_a), 3.85 (s, 12H, OMe), 3.97–0.85 (m, 28H, f + g + k). Conformational isomer 3C4R_B·4PF₆: ¹H NMR (600 MHz, CD₃CN) δ 8.62 (d, J = 6.5 Hz, 4H, α), 8.16 (bs, 4H, NH₂), 7.96 (s, 2H, OH), 7.82 (s, 2H, OH), 7.51 (s, 2H, OH), 7.39 (s, 2H, OH), 7.21 (s, 2H, ArH), 7.18 (s, 2H, ArH), 7.16 (s, 2H, OH), 6.93 (m, 4H, b), 6.68 (s, 2H, ArH), 6.56 (m, 2H, a), 6.50 (s, 2H, e), 6.39 (s, 2H, ArH), 6.22 (s, 2H, ArH), 5.95–5.71 (m, 24H, x_a + x_b), 5.71 (d, J = 6.5 Hz, 4H, β), 5.33 (s, 24H, z), 4.80 (m, 4H, h), 4.44–4.39 (m, 8H, c and d), 4.24 (d, J = 15.2 Hz, 12H, y_b), 4.11 (d, J = 15.2 Hz, 12H, y_a), 3.85 (s, 12H, OMe), 3.97–0.85 (m, 28H, f + g + k). Conformational isomer 3C4R_C·4PF₆: ¹H NMR (600 MHz, CD₃CN) δ 8.60 (d, J = 6.5 Hz, 4H, α), 8.16 (bs, 4H, NH₂), 8.05 (s, 2H, OH), 7.99 (s, 2H, OH), 7.68 (s, 2H, OH), 7.23 (s, 2H, OH), 7.23 (s, 2H, OH), 7.10 (s, 2H, ArH), 6.98 (s, 2H, ArH), 6.93 (m, 4H, b), 6.56 (m, 2H, a), 6.53 (s, 2H, ArH), 6.51 (s, 2H, ArH), 6.51 (s, 2H, ArH), 6.50 (s, 2H, e), 5.95–5.71 (m, 24H, x_a + x_b), 5.87 (d, J = 6.5 Hz, 4H, β), 5.33 (s, 24H, z), 4.80 (m, 4H, h), 4.44–4.39 (m, 8H, c and d), 4.24 (d, J = 15.2 Hz, 12H, y_b), 4.11 (d, J = 15.2 Hz, 12H, y_a), 3.85 (s,

12H, OMe), 3.97–0.85 (m, 28H, f + g + k). Conformational isomer 3C4R_D·4PF₆: ¹H NMR (600 MHz, CD₃CN) δ 8.74 (d, J = 6.5 Hz, 4H, α), 8.16 (bs, 4H, NH₂), 8.19 (s, 2H, OH), 8.19 (s, 2H, OH), 7.95 (s, 2H, OH), 7.64 (s, 2H, OH), 7.60 (s, 2H, OH), 7.14 (s, 2H, ArH), 6.93 (m, 4H, b), 6.90 (s, 2H, ArH), 6.56 (m, 2H, a), 6.50 (s, 2H, e), 6.40 (s, 2H, ArH), 6.26 (s, 2H, ArH), 6.26 (s, 2H, ArH), 5.95–5.71 (m, 24H, x_a + x_b), 5.54 (d, J = 6.5 Hz, 4H, β), 5.33 (s, 24H, z), 4.80 (m, 4H, h), 4.44–4.39 (m, 8H, c and d), 4.24 (d, J = 15.2 Hz, 12H, y_b), 4.11 (d, J = 15.2 Hz, 12H, y_a), 3.85 (s, 12H, OMe), 3.97–0.85 (m, 28H, f + g + k).

4C5R_{AA}·4TFA. 4CV·2PF₆ (25 mg, 39 μmol, 1.0 equiv) and P (60 mg, 98 μmol, 2.5 equiv) were mixed in MeCN (30 mL) and stirred at 55 °C for 30 min before [1CCB] (140 mg, 98 μmol, 2.5 equiv) was added. The reaction was monitored by TLC (SiO₂: Me₂CO with 2% NH₄PF₆ (m/v), I₂ stain, R_f = 0.28). After all the 4CV·2PF₆ had been consumed, the solvent was removed, and the residue was purified by column chromatography (SiO₂: Me₂CO with 0.3% NH₄PF₆ and then Me₂CO with 2% NH₄PF₆ (m/v)). The fraction with R_f = 0.28 (TLC/SiO₂: Me₂CO with 2% NH₄PF₆ (m/v)) was collected and the solvent was removed under the reduced pressure. H₂O (20 mL) was added to the residue to remove excess of NH₄PF₆, whereupon the product "crashed out" as an orange precipitate. The solid was collected by filtration, washed with an excess of H₂O to remove NH₄PF₆, and dried under high vacuum to afford 4C5R·4PF₆ as a light orange powder (yield 59%). In the case of the hetero[5]rotaxane 4C5R·4PF₆, while several isomers are observed, it is high impossible assign them to each of the four different conformational isomers of P rings on the dumbbell. When the separation of the conformational isomers was attempted using recycling reversed-phase HPLC (H₂O/MeCN (0.1% TFA) = 80: 20 to 60: 40 in 40 min, flow rate: 17 mL/min), three major fractions were collected (see the Supporting Information). Only one fraction was obtained pure (fraction 2, yield 80%) and the conformation was assigned to one in which both P rings adopt a C₅ conformation, namely 4C5R_{AA}·4TFA, resulting from an analysis of the ¹H NMR spectrum together with the 2D ¹H-¹H COSY, ¹H-¹³C HSQC, and ¹H-¹H NOESY spectra (see the Supporting Information): ¹H NMR (600 MHz, (CD₃)₂SO, 298 K) δ 8.96 (s, 10H), 8.80 (s, 10H), 7.53 – 7.38 (m, 4H), 7.34 (s, 4H), 7.25 (d, J = 6.0 Hz, 4H), 7.08 (d, J = 2.3 Hz, 4H), 6.73 (s, 10H), 6.54 (t, J = 2.3 Hz, 2H), 6.49 (s, 2H), 5.82 (d, J = 15.2 Hz, 12H), 5.63 (d, J = 14.9 Hz, 12H), 5.54 (s, 24H), 4.67 (d, J = 5.9 Hz, 4H), 4.52 (d, J = 15.1 Hz, 12H), 4.39 (d, J = 14.0 Hz, 12H), 4.36 – 4.21 (m, 8H), 3.88 (m, 4H), 3.85 (s, 12H), 3.63 (bs, 20H), 3.03 (m, 4H), 2.33 – 2.14 (m, 4H), 1.05 (m, 4H); ¹³C NMR (125 MHz, (CD₃)₂SO, 298 K) δ = 160.0, 157.6, 155.8, 155.5, 147.9, 145.0, 143.0, 136.2, 133.7, 127.7, 126.2, 124.3, 118.7, 118.3, 117.3, 107.9, 101.0, 69.4, 69.3, 61.9, 55.2, 52.8, 50.8, 50.4, 50.0, 43.2, 28.4, 26.9, 23.3, 22.5; HR-ESI-MS calcd for [M - 4PF₆ + 4H]⁴⁺ m/z = 994.6014, found m/z = 994.6042, [M - 4PF₆ + 3H]³⁺ m/z = 1325.4651, found m/z = 1325.4667.

■ ASSOCIATED CONTENT

● Supporting Information

Full details of instrumentation and analytical techniques; synthesis and characterization data for the [4]- and [5]-rotaxanes 2C4R–5C5R·4PF₆ and their precursors; ¹H-¹H COSY, NOESY, ¹H-¹³C HSQC and variable-temperature ¹H NMR spectroscopic investigation of the [4]rotaxanes 2C4R–3C4R·4PF₆; UV–vis absorption spectra of 2C4R–5C5R·4PF₆ and 2C3R·4PF₆; high-resolution mass spectra of [4]- and [5]rotaxanes 2C4R–5C5R·4PF₆ and their precursors; partially resolved crystal data and molecular modeling of the [4]- and [5]rotaxane using molecular dynamics and energy minimization. This material is available free of charge via the Internet at <http://pubs.acs.org>.

■ AUTHOR INFORMATION

Corresponding Author

stoddart@northwestern.edu

Notes

The authors declare no competing financial interest.

■ ACKNOWLEDGMENTS

This work was performed under the auspices of the King Abdulaziz City of Science and Technology (KACST) and Northwestern University (NU) Joint Center of Excellence for Integrated NanoSystems (JCEINS). We thank Drs. Turki S. Saud and Nezar H. Khadry for their interest in the research. C.K. thanks the Royal Society in the UK for support as a Newton Fellow Alumnus (Follow-on Scheme 2012–2013). N.L.S. thanks NSF for a Graduate Research Fellowship. P.R.M. thanks the US–UK Fulbright Commission for an All Disciplines Scholar Award.

■ REFERENCES

- (1) (a) Villà, J.; Warshel, A. *J. Phys. Chem. B* **2001**, *105*, 7887. (b) Olsson, M. H. M.; Parson, W. W.; Warshel, A. *Chem. Rev.* **2006**, *106*, 1737.
- (2) For a review, see: Dong, Z. Y.; Luo, Q.; Liu, J. Q. *Chem. Soc. Rev.* **2012**, *41*, 7890.
- (3) (a) Chevallier, F.; Breit, B. *Angew. Chem., Int. Ed.* **2006**, *45*, 1599. (b) Waloch, C.; Wieland, J.; Keller, M.; Breit, B. *Angew. Chem., Int. Ed.* **2007**, *46*, 3037.
- (4) (a) Anslyn, E.; Breslow, R. *J. Am. Chem. Soc.* **1989**, *111*, 8931. (b) Breslow, R. *Acc. Chem. Res.* **1995**, *28*, 146. (c) Kirby, A. J. *Angew. Chem., Int. Ed.* **1996**, *35*, 707.
- (5) (a) Kang, J. M.; Rebek, J., Jr. *Nature* **1997**, *385*, 50. (b) Yoshizawa, M.; Tamura, M.; Fujita, M. *Science* **2006**, *312*, 251. (c) Wang, Z. J.; Clary, K. N.; Bergman, R. G.; Raymond, K. N.; Toste, F. D. *Nat. Chem.* **2013**, *5*, 100.
- (6) (a) Yang, C.; Nakamura, A.; Fukuhara, G.; Origane, Y.; Mori, T.; Wada, T.; Inoue, Y. *J. Org. Chem.* **2006**, *71*, 3126. (b) Yang, C.; Mori, T.; Inoue, Y. *J. Org. Chem.* **2008**, *73*, 5786. (c) Yang, C.; Mori, T.; Origane, Y.; Ko, Y. H.; Selvapalam, N.; Kim, K.; Inoue, Y. *J. Am. Chem. Soc.* **2008**, *130*, 8574. (d) Ke, C. F.; Yang, C.; Mori, T.; Wada, T.; Liu, Y.; Inoue, Y. *Angew. Chem., Int. Ed.* **2009**, *48*, 6675. (e) Yang, C.; Ke, C. F.; Liang, W. T.; Fukuhara, G.; Mori, T.; Liu, Y.; Inoue, Y. *J. Am. Chem. Soc.* **2011**, *133*, 13786.
- (7) Amirsakis, D. G.; Garcia-Garibay, M. A.; Rowan, S. J.; Stoddart, J. F.; White, A. J. P.; Williams, D. J. *Angew. Chem., Int. Ed.* **2001**, *40*, 4256.
- (8) (a) Fiedler, D.; Leung, D. H.; Bergman, R. G.; Raymond, K. N. *Acc. Chem. Res.* **2005**, *38*, 349. (b) Fujita, M.; Tominaga, M.; Hori, A.; Therrien, B. *Acc. Chem. Res.* **2005**, *38*, 369. (c) Pluth, M. D.; Bergman, R. G.; Raymond, K. N. *Science* **2007**, *316*, 85. (d) Nishioka, Y.; Yamaguchi, T.; Yoshizawa, M.; Fujita, M. *J. Am. Chem. Soc.* **2007**, *129*, 7000. (e) Nishioka, Y.; Yamaguchi, T.; Kawano, M.; Fujita, M. *J. Am. Chem. Soc.* **2008**, *130*, 8160. (f) Hastings, C. J.; Backlund, M. P.; Bergman, R. G.; Raymond, K. N. *Angew. Chem., Int. Ed.* **2011**, *50*, 10570.
- (9) (a) Bakirci, H.; Koner, A. L.; Dickman, M. H.; Kortz, U.; Nau, W. M. *Angew. Chem., Int. Ed. Engl.* **2006**, *45*, 7400. (b) Cacciapaglia, R.; Di Stefano, S.; Kelderman, E.; Mandolini, L. *Angew. Chem., Int. Ed.* **1999**, *38*, 348. (c) Komiyama, M.; Kina, S.; Matsumura, K.; Sumaoka, J.; Tobey, S.; Lynch, V. M.; Anslyn, E. *J. Am. Chem. Soc.* **2002**, *124*, 13731. (d) Cacciapaglia, R.; Casnati, A.; Mandolini, L.; Reinhoudt, D. N.; Salvio, R.; Sartori, A.; Ungaro, R. *J. Am. Chem. Soc.* **2006**, *128*, 12322. (e) Nwe, K.; Andolina, C. M.; Morrow, J. R. *J. Am. Chem. Soc.* **2008**, *130*, 14861.
- (10) (a) Jon, S. Y.; Ko, Y. H.; Park, S. H.; Kim, H. J.; Kim, K. *Chem. Commun.* **2001**, 1938. (b) Pattabiraman, M.; Natarajan, A.; Kaliappan, R.; Mague, J. T.; Ramamurthy, V. *Chem. Commun.* **2005**, 4542.
- (c) Wang, R. B.; Yuan, L. N.; Macartney, D. H. *J. Org. Chem.* **2006**, *71*, 1237. (d) Lu, X. Y.; Masson, E. *Org. Lett.* **2010**, *12*, 2310. (e) Koner, A. L.; Márquez, C.; Dickman, M. H.; Nau, W. M. *Angew. Chem., Int. Ed.* **2011**, *50*, 545.
- (11) (a) Mock, W. L.; Irra, T. A.; Wepsiec, J. P.; Manimaran, T. L. *J. Org. Chem.* **1983**, *48*, 3619. (b) Mock, W. L.; Irra, T. A.; Wepsiec, J. P.; Adhya, M. J. *Org. Chem.* **1989**, *54*, 5302.
- (12) (a) Huisgen, R.; Szeimies, G.; Möbius, L. *Chem. Ber.* **1967**, *100*, 2494. (b) Bastide, J.; Hamelin, J.; Texier, F.; Quang, Y. V. *Bull. Soc. Chim. Fr.* **1973**, 2555. (c) Bastide, J.; Hamelin, J.; Texier, F.; Quang, Y. V. *Bull. Soc. Chim. Fr.* **1973**, 2871. (d) Huisgen, R. *Pure Appl. Chem.* **1989**, *61*, 613.
- (13) (a) Kolb, H. C.; Finn, M. G.; Sharpless, K. B. *Angew. Chem., Int. Ed.* **2001**, *40*, 2004. (b) Rostovtsev, V. V.; Green, L. G.; Fokin, V. V.; Sharpless, K. B. *Angew. Chem., Int. Ed.* **2002**, *41*, 2596. (c) Tornøe, C. W.; Christensen, C.; Meldal, M. *J. Org. Chem.* **2002**, *67*, 3057.
- (14) (a) Tuncel, D.; Steinke, J. H. G. *Chem. Commun.* **1999**, 1509. (b) Tuncel, D.; Steinke, J. H. G. *Chem. Commun.* **2001**, 253. (c) Tuncel, D.; Steinke, J. H. G. *Chem. Commun.* **2002**, 496. (d) Tuncel, D.; Steinke, J. H. G. *Macromolecules* **2004**, *37*, 288. (e) Tuncel, D.; Ünal, O.; Artar, M. *Isr. J. Chem.* **2011**, *51*, 525.
- (15) (a) Tuncel, D.; Tiftik, H. B.; Salih, B. *J. Mater. Chem.* **2006**, *16*, 3291. (b) Tuncel, D.; Özsar, O.; Tiftik, H. B.; Salih, B. *Chem. Commun.* **2007**, 1369. (c) Tuncel, D.; Katterle, M. *Chem.—Eur. J.* **2008**, *14*, 4110. (d) Celtek, G.; Artar, M.; Scherman, O. A.; Tuncel, D. *Chem.—Eur. J.* **2009**, *15*, 10360. (e) Hänni, K. D.; Leigh, D. A. *Chem. Soc. Rev.* **2010**, *39*, 1240.
- (16) Angelos, S.; Yang, Y. W.; Patel, K.; Stoddart, J. F.; Zink, J. I. *Angew. Chem., Int. Ed.* **2008**, *47*, 2222.
- (17) (a) Lee, J. W.; Samal, S.; Selvapalam, N.; Kim, H.-J.; Kim, K. *Acc. Chem. Res.* **2003**, *36*, 621. (b) Lagona, J.; Mukhopadhyay, P.; Chakrabarti, S.; Isaacs, L. *Angew. Chem., Int. Ed.* **2005**, *44*, 4844. (c) Liu, S.; Ruspic, C.; Mukhopadhyay, P.; Chakrabarti, S.; Zavalij, P. Y.; Isaacs, L. *J. Am. Chem. Soc.* **2005**, *127*, 15959.
- (18) CB can be introduced into aqueous solution in the presence of alkaline earth metal or ammonium ions.
- (19) Yin, J.; Chi, C.; Wu, J. *Org. Biomol. Chem.* **2010**, *8*, 2594.
- (20) Carlqvist, P.; Maseras, F. *Chem. Commun.* **2007**, 748.
- (21) (a) Biedermann, F.; Uzunova, V. D.; Scherman, O. A.; Nau, W. M.; De Simone, A. *J. Am. Chem. Soc.* **2012**, *134*, 15318. (b) Nguyen, C. N.; Young, T. K.; Gilson, M. K. *J. Chem. Phys.* **2012**, *137*, 149901.
- (22) (a) Rekharsky, M. V.; Yamamura, H.; Kawai, M.; Osaka, I.; Arakawa, R.; Sato, A.; Ko, Y. H.; Selvapalam, N.; Kim, K.; Inoue, Y. *Org. Lett.* **2006**, *8*, 815. (b) Rekharsky, M. V.; Ko, Y. H.; Selvapalam, N.; Kim, K.; Inoue, Y. *Supramol. Chem.* **2007**, *19*, 39. (c) Kim, Y.; Kim, H.; Ko, Y. H.; Selvapalam, N.; Rekharsky, M. V.; Inoue, Y.; Kim, K. *Chem.—Eur. J.* **2009**, *15*, 6143.
- (23) Ke, C.; Smaldone, R. A.; Kikuchi, T.; Li, H.; Davis, A. P.; Stoddart, J. F. *Angew. Chem., Int. Ed.* **2013**, *52*, 381.
- (24) Positive cooperativity has also been observed during the template-directed syntheses of oligorotaxanes involving $-CH_2NH_2^+CH_2-$ centers and [24]crown-8 macrocycles. See: (a) Belowich, M. E.; Valente, C.; Stoddart, J. F. *Angew. Chem., Int. Ed.* **2010**, *49*, 7208. (b) Belowich, M. E.; Valente, C.; Smaldone, R. A.; Friedman, D. C.; Thiel, J.; Cronin, L.; Stoddart, J. F. *J. Am. Chem. Soc.* **2012**, *134*, 5243. (c) Avestro, A.-J.; Belowich, M. E.; Stoddart, J. F. *Chem. Soc. Rev.* **2012**, *41*, 5881.
- (25) (a) Whitty, A. *Nat. Chem. Biol.* **2008**, *4*, 435. (b) Hunter, C. A.; Anderson, H. L. *Angew. Chem., Int. Ed.* **2009**, *48*, 7488. (c) Ercolani, G.; Schiaffino, L. *Angew. Chem., Int. Ed.* **2011**, *50*, 1762.
- (26) (a) Ogoshi, T.; Kanai, S.; Fujinami, S.; Yamagishi, T. A.; Nakamoto, Y. *J. Am. Chem. Soc.* **2008**, *130*, 5022. (b) Cao, D. R.; Kou, Y. H.; Liang, J. Q.; Chen, Z. Z.; Wang, L. Y.; Meier, H. *Angew. Chem., Int. Ed.* **2009**, *48*, 9721. (c) Ogoshi, T.; Aoki, T.; Shiga, R.; Iizuka, R.; Ueda, S.; Demachi, K.; Yamafuji, D.; Kayama, H.; Yamagishi, T. A. *J. Am. Chem. Soc.* **2012**, *134*, 20322. (d) Han, C. Y.; Zhang, Z. B.; Chi, X. D.; Zhang, M. M.; Yu, G. C.; Huang, F. H. *Acta. Chim. Sinica* **2012**, *70*, 1775. (e) Chen, Y.; Tao, H. Q.; Kou, Y. H.; Meier, H.; Fu, J. L.; Cao, D. R. *Chin. Chem. Lett.* **2012**, *23*, 509. (f) Hu, X. B.; Chen, Z. X.; Chen,

L.; Zhang, L.; Hou, J. L.; Li, Z. T. *Chem. Commun.* **2012**, 48, 10999. (g) Ogoshi, T.; Shiga, R.; Yamagishi, T. *J. Am. Chem. Soc.* **2012**, 134, 4577. (h) Ogoshi, T.; Aoki, T.; Kitajima, K.; Fujinami, S.; Yamagishi, T.; Nakamoto, Y. *J. Org. Chem.* **2011**, 76, 328.

(27) In engineering, a gasket is a shaped piece or ring of material which is sandwiched between matched machine parts or matching pipes to provide a seal. Gaskets often have a degree of elasticity which allows a robust joint to form between two surfaces that, as a result of imperfections or slight size mismatch, might not fit together perfectly. In the chemical analogue discussed in this paper, the P rings act as gaskets by facilitating the reaction of substrates that do not match the strict length requirements usually imposed by the CB-AAC; this length mismatch arises from inter-ring hydrogen bonds between CB and P, forming a kind of noncovalent joint, which stabilize otherwise unfavorable co-conformations in the multicomponent assemblies.

(28) (a) Ajami, D.; Rebek, J. *J. Am. Chem. Soc.* **2006**, 128, 5314. (b) Tiefenbacher, K.; Ajami, D.; Rebek, J. *Angew. Chem., Int. Ed.* **2011**, 50, 12003.

(29) Hunter, C. A. *Angew. Chem., Int. Ed.* **2004**, 43, 5310.

(30) It is worth noting that pillar[6]arene adopts the same C_6 symmetry as cucurbit[6]uril. Their rim sizes, however, are not complementary. Molecular mechanical simulation experiments show that the pillar[5]arene is a better candidate for P-CB-AAC.

(31) Yin, J.; Chi, C. Y.; Wu, J. S. *Chem.—Eur. J.* **2009**, 15, 6050.

(32) The same strategy was not successful in the making the rod precursor $2CV^{2+}$ -CCB complex using counterion exchange, most likely because the cation-dipole interaction between $2CV\cdot 2PF_6$ and CB is not strong enough.

(33) Buschmann, H.-J.; Cleve, E.; Jansen, K.; Wego, A.; Schollmeyer, E. *J. Inclusion Phenom. Macrocyclic Chem.* **2001**, 40, 117.

(34) *N*-(3,5-Dimethoxybenzyl)propargylammonium chloride (1-Cl) is not large enough to prevent the P ring from dethreading from the dumbbell. It is able, however, to prevent the CB ring from dethreading. Thus, the CB ring and 3,5-dimethoxyphenyl groups act together as an integral stopper for the P ring.

(35) (a) Ogoshi, T.; Nishida, Y.; Yamagishi, T. A.; Nakamoto, Y. *Macromolecules* **2010**, 43, 7068. (b) Li, C. J.; Xu, Q. Q.; Li, J.; Yao, F. N.; Jia, X. S. *Org. Biomol. Chem.* **2010**, 8, 1568. (c) Ogoshi, T.; Tanaka, S.; Yamagishi, T.; Nakamoto, Y. *Chem. Lett.* **2011**, 40, 96. (d) Ogoshi, T.; Yamafuji, D.; Aoki, T.; Yamagishi, T. *J. Org. Chem.* **2011**, 76, 9497. (e) Strutt, N. L.; Forgan, R. S.; Spruell, J. M.; Botros, Y. Y.; Stoddart, J. F. *J. Am. Chem. Soc.* **2011**, 133, 5668. (f) Strutt, N. L.; Fairen-Jimenez, D.; Iehl, J.; Lalonde, M. B.; Snurr, R. Q.; Farha, O. K.; Hupp, J. T.; Stoddart, J. F. *J. Am. Chem. Soc.* **2012**, 134, 17436. (g) Strutt, N. L.; Zhang, H. C.; Giesener, M. A.; Lei, J. Y.; Stoddart, J. F. *Chem. Commun.* **2012**, 48, 1647.

(36) Similar binding behavior of cucurbiturils with bipyridinium ($BIPY^{2+}$) and secondary ammonium (NH_2^+) derivatives has been widely reported. See a recent review: Masson, E.; Ling, X. X.; Joseph, R.; Kyeremeh-Mensah, L.; Lu, X. Y. *RSC Adv.* **2012**, 2, 1213.

(37) To date, no successful example has been reported for the CB-templated reaction, other than that employing propargylammonium and azidoethylammonium functions.

(38) The two binding sites at each portal of CB are occupied by two of the stopper precursor 1^{2+} .

(39) For a quick demonstration, we have also carried out several preliminary test reactions. See the Supporting Information.

(40) A Job plot of $4CV\cdot 2PF_6$ (see the Supporting Information) with P reveals that both 1:1 and 1:2 binding modes occur in solution. On account of the solubility of the complex, the Job plot measurement was performed in $(CD_3)_2CO$.

(41) (a) Ogoshi, T.; Kitajima, K.; Yamagishi, T. A.; Nakamoto, Y. *Org. Lett.* **2010**, 12, 636. (b) Ogoshi, T.; Kitajima, K.; Aoki, T.; Fujinami, S.; Yamagishi, T.; Nakamoto, Y. *J. Org. Chem.* **2010**, 75, 3268. (c) Ogoshi, T.; Masaki, K.; Shiga, R.; Kitajima, K.; Yamagishi, T. *Org. Lett.* **2011**, 13, 1264. (d) Ogoshi, T.; Shiga, R.; Yamagishi, T.; Nakamoto, Y. *J. Org. Chem.* **2011**, 76, 618. (e) Xue, M.; Yang, Y.; Chi, X. D.; Zhang, Z. B.; Huang, F. H. *Acc. Chem. Res.* **2012**, 45, 1294.

(42) Ogoshi, T.; Kitajima, K.; Aoki, T.; Yamagishi, T.; Nakamoto, Y. *J. Phys. Chem. Lett.* **2010**, 1, 817.

(43) Strictly speaking, the term “conformation” refers only to discrete molecular species. We have used “co-conformation” to designate the three-dimensional spatial arrangement of the atoms in supramolecular systems. See: Fyfe, M. C. T.; Glink, P. T.; Menzer, S.; Stoddart, J. F.; White, A. J. P.; Williams, D. J. *Angew. Chem., Int. Ed. Engl.* **1997**, 36, 2068–2070. In this study, CB and P rings encircle their correspondent binding site, the triazole ring and $BIPY^{2+}$ unit, respectively, in the dumbbell of the hetero[4]- and [5]rotaxanes. The co-conformation of the hetero[4]- and [5]rotaxanes are fixed by the hydrogen bonding networks formed between CB and P rings. The conformations of P rings on the dumbbell components of the rotaxanes represent their three-dimensional spatial arrangements. Consequently, we have used the term conformational isomer to differentiate the hetero[4]- and [5]rotaxanes with different conformations of the P rings on the dumbbell components.

(44) The resonances of P do not exchange in the variable temperature (VT) 1H NMR spectroscopic investigations even when heating up to 100 °C. See the Supporting Information for details.

(45) Conformational isomer D is the most thermodynamically stable conformation of P by itself on account of an intraring hydrogen-bonding network.

(46) Counterions were omitted from the model for the sake of simplicity. See the Supporting Information for overlaid structures.

(47) Day, A.; Arnold, A. P.; Blanch, R. J.; Snushall, B. *J. Org. Chem.* **2001**, 66, 8094.

(48) Li, H.; Zhu, Z.; Fahrenbach, A. C.; Savoie, B. M.; Ke, C.; Barnes, J. C.; Lei, J.; Zhao, Y. L.; Lilley, L. M.; Marks, T. J.; Ratner, M. A.; Stoddart, J. F. *J. Am. Chem. Soc.* **2013**, 135, 456.